CALIBRATING ANTENNA STANDARDS USING CW AND PULSED-CW MEASUREMENTS AND THE PLANAR NEAR-FIELD METHOD

D. P. Kremer and A. G. Repjar

Electromagnetic Fields Division 723.05
National Bureau of Standards
Boulder, Colorado 80303 U.S.A.

Abstract

For over a decade the National Bureau of Standards (NBS) has used the planar near-field method to accurately determine the gain, polarization and patterns of antennas either transmitting or receiving cw signals. Some of these calibrated antennas have also been measured at other facilities to determine and/or verify the accuracies obtainable with their ranges. The facilities involved have included near-field ranges, far-field ranges, and compact ranges.

Recently, NBS has calibrated an antenna to be used to evaluate both a near-field range and a compact range. These ranges are to be used to measure an electronically-steerable antenna which transmits only pulsed-cw signals. The antenna calibrated by NBS was chosen to be similar in physical size and frequency of operation to the array and was also calibrated with the antenna transmitting pulsed-cw. This calibration included determining the effects of using different power levels at the mixer, the accuracy of the receiver in making the amplitude and phase measurements, and the effective dynamic range of the receiver. Comparisons were made with calibration results obtained for the antenna transmitting cw and for the antenna receiving cw. The parameters compared include gain, sidelobe and cross polarization levels. The measurements are described and some results are presented.

INTRODUCTION

The National Bureau of Standards (NBS) has often calibrated antennas which have been used to evaluate the accuracy of other measurement ranges including near-field ranges, far-field ranges and compact ranges. These antennas are especially important for evaluating the latter two ranges where the error analyses are difficult, incomplete or both. The antennas under test at these other ranges were measured either transmitting cw or receiving cw as were the antennas calibrated at NBS. Recently there has been a need for ranges to measure electronically-steerable array antennas which transmit only pulsed-cw. The receiving systems thus must have the capability of measuring pulsed-cw accurately and the ranges must be able to measure the antennas' parameters over a wide range of steering angles.

NBS has recently completed the calibration of an antenna transmitting pulsed-cw using its planar near-field range. This antenna will be used to evaluate both a near-field range and compact range at other facilities where an antenna of similar size and frequency of operation will be calibrated. The accuracy of this calibration was evaluated by comparing the results with those obtained by measuring the same antenna first transmitting cw and then receiving cw. The important effects due to the dynamic range of the receiver when used in the pulsed-cw mode, due to scan area truncation, and due to multiple reflection signals were determined. The purpose of this paper is to describe the measurements, discuss the problems encountered and the error budgets, and present some results.

TEST PLAN

The power gains and patterns of an X-band array, approximately 90 cm in diameter, were measured on the NBS indoor range using the planar near-field scanning technique. The antenna was aligned by following the necessary procedure outlined in the notes for the planar near-field measurements short course [1]. First the antenna was measured transmitting cw (Xmit cw). This is the most common procedure used at the NBS near-field facility. Second, the antenna was measured transmitting pulsed-cw with a 10% duty cycle (pulsed-cw 1). The power levels were unchanged from the first measurement so that the mixer would not be overdriven. Third the antenna was measured transmitting pulsed-cw but the power level was increased by 10 dB so that the full dynamic range of the receiver might be used (pulsed-cw 2). Finally the antenna was measured receiving cw (Recv cw).

For the planar near-field technique, reports that describe this method in detail are available [1-10]. Briefly, the method consists of measuring the complex near field (amplitude and phase) of the test antenna over a plane area with a probe antenna whose characteristics are known. The near field is measured for two orientations of the probe antenna and then these data are processed by computer to obtain the main and cross linear polarization components of the far field for the test antenna. This processing includes correcting for the effects of the probe. Far-field gain is then calculated and patterns generated. For this measurement, the probe antenna was an X-band open-ended waveguide probe that had previously been calibrated on the NBS pattern range.

The near-field measurements were conducted at two separation distances between the probe and test antenna to evaluate scan truncation effects. The first distance chosen was 30 cm or about 10 wavelengths and was based on multipath testing. Both truncation effects and multipath tests are discussed in [1]. The second distance was 12 cm or about 4 wavelengths and was chosen to determine if accurate results could be obtained at a closer distance using a smaller measurement area.

Two measurement areas, nominally 140 cm by 140 cm and 180 cm by 180 cm were used. These resulted in near-field measurement arrays of 111x111 and 143x143 respectively since the sampling interval was 1.27 cm. This interval is less than one-half wavelength as required by the sampling theorem [1]. Both theory [7] and empirical results [8] have shown that for directive antennas, the primary effect of reducing the measurement area is to restrict the angular region where the results are valid. For a scan length L, antenna diameter D, and separation distance d, the results are valid for angles

$$A < A_c = \tan^{-1}[(L - D)/2d]. \qquad (1)$$

RESULTS

Although the primary results desired are direct pattern comparisons for the measurements described above along with comparisons to results obtained at another smaller near-field facility, on-axis gain results are indicative of pattern agreements. These results are summarized in tables 1-4 along with the angles of validity of the far-field patterns. The uncertainties for the gain measurements are a quadrature sum (RSS) of each of the error components listed in table 5. Each component is either a worst-case or 3-sigma value, and is assumed to be independent of other errors. The differences in the gain uncertainties in tables 1-4 were calculated as shown in table 5. For the pulsed-cw 2 case, an amplifier was utilized to obtain the additional 10 dB power needed to use the full dynamic range of the receiver. In the course of our data reduction, it was determined that the amplifier was non-linear. That is, its gain was dependent on its input power. This amplifier non-linearity also affected the accuracy of the receiver non-linearity measurement. In the future these two uncertainties will be reduced.

Table 1. Measured antenna gain at 9.7 GHz. Input array size is 111x111. A_c = 62 deg.

Condition		AUT/probe separation (cm)	On-axis Gain (dB)
Xmit	cw	12	36.56 ± 0.21
Xmit	pulsed-cw 1	12	36.54 ± 0.21
Xmit	pulsed-cw 2	12	36.79 ± 0.39
Recv	cw	12	36.75 ± 0.21

Table 2. Measured antenna gain at 9.7 GHz. Input array size is 111x111. A_c = 38 deg.

Condition		AUT/probe separation (cm)	On-axis Gain (dB)
Xmit	cw	30	36.56 ± 0.21
Xmit	pulsed-cw 1	30	36.54 ± 0.21
Xmit	pulsed-cw 2	30	36.60 ± 0.39
Recv	cw	30	36.57 ± 0.21

Table 3. Measured antenna gain at 9.7 GHz. Input array size is 143x143. A_c = 74 deg.

Condition		AUT/probe separation (cm)	On-axis Gain (dB)
Xmit	cw	12	36.57 ± 0.21
Xmit	pulsed-cw 1	12	36.53 ± 0.21
Xmit	pulsed-cw 2	12	36.92 ± 0.39
Recv	cw	12	36.75 ± 0.21

Table 4. Measured antenna gain at 9.7 GHz. Input array size is 143x143. A_c = 56 deg.

Condition		AUT/probe separation (cm)	On-axis Gain (dB)
Xmit	cw	30	36.67 ± 0.21
Xmit	pulsed-cw 1	30	36.70 ± 0.21
Xmit	pulsed-cw 2	30	36.76 ± 0.39
Recv	cw	30	36.61 ± 0.21

Table 5. Uncertainties in gain measurements.

Source of error Type	Resultant error cw. pulsed-cw 1	pulsed-c
Systematic		
Receiver non-linearity	0.06	0.15
Probe gain uncertainty	0.15	0.15
Normalization amplitude	0.10	0.10
Multiple reflections	0.07	0.07
Mismatch error	<0.01	<0.01
Antenna alignment	0.02	0.02
Flange errors	0.02	0.02
Position errors	<0.01	<0.01
Area truncation	<0.01	<0.01
Amplifier errors		0.30
Random		
Normalization amplitude	0.06	0.06
Relative amplitudes and phases	≤0.01	≤0.01
	±0.21	±0.39

The maximum differences in the gain values for tables 1-4 are 0.23, 0.06, 0.35, and 0.15 dB respectively. As mentionned earlier the optimum separation distance between the probe and the antenna based on multipath testing is 30 cm. For this reason the gains in tables 2 and 4 have the smaller maximum differences. Also by comparing tables 1 and 3, we see that the maximum difference in the gain values as a function of truncation is 0.13 dB for the pulsed-cw 2 condition. Therefore by considering all the measurements, we see that multipath effects result in a greater difference in the gain values than truncation effects. With differences of these magnitudes, we would expect the antenna patterns in the main beam region for the main component to agree quite closely. This will be shown below.

The far-field probe-corrected patterns of the antenna are shown in figures 1-9. The abscissas of each graph are normalized k-space values. Typical main component results are given in figures 1a and 1b where the E- and H-plane far-field patterns respectively are compared for different conditions. This figure shows the excellent pattern agreement alluded to earlier. Results for the cross component are given in figure 2. The small effects of scan area truncation for the main and cross components can be seen in figures 3 and 4 respectively. Comparisons of the antenna patterns shown in figure 5, calculated from data taken at the two different d distances, indicate that there are some small differences in the sidelobe levels of the main component and in the levels of the cross component. Results shown in figure 6 suggests that these differences are due to multiple reflections.

For the pulsed-cw measurements (10% duty cycle), the full dynamic range of the receiver can be used to obtain more accurate main and cross component results. This was accomplished by increasing the power level by 10 dB to overdrive the mixer and then correcting for the resulting non-linearity in the receiving system response by its calibration using a precision rotary vane attenuator. The effects of this correction for the cross component can be clearly seen by comparing figures 2 and 7. Specifically, the noise floors in figure 2 are substantially less than those in figure 7.

The effects of scan area truncation are in accord with those expected by applying eq 1. Figure 3 shows good agreement for normalized k values less than 0.88 (A_c = 62 deg.) for the ca[se] where the near-field data were taken [at] the closer distance, d = 12 cm, and A[$_c$] is reduced from 74 to 62 deg. Figure [4] shows good agreement only for normalized k values less than 0.62 (A_c = 38 deg.) for the case where the data were taken at the further distance, d = 30 cm and A_c is reduced from 56 to 38 deg.

Comparisons with patterns measured at another facility for the main component of the antenna standard show an excellent agreement particularly if we allow for the small differences expected from multiple reflection effects (figure 9). Cross component data were not taken by the other facility, hence comparisons could not be made.

CONCLUSIONS

The on-axis gain results confirm that good pattern agreements are obtained in the main-beam regions for the main component. Second, the effects of scan area truncation are in accord with those expected by theory. Third, this antenna standard can be effectively used to evaluate other antenna ranges since accurate gain, sidelobe and cross polarization levels were obtained. However, the antennas to be evaluated should be similar in electrical size, frequency and operation to this standard. Finally, two problems still need to be addressed when an antenna standard is electronically-steerable. Truncation effects need to be evaluated when the antenna is steered to wide angles, and the effects of multiple reflections between the probe and the antenna need to be determined.

REFERENCES

[1] Newell, A. C. Planar near-field measurements. Short Course Notes. NBS, Boulder, Colorado; June 1985.

[2] Kerns, D. M.; Dayhoff, E. S. Theory of diffraction in microwave interferometry. Nat. Bur. Stand. (U.S.) J. Res. 64(B): 1-13; Jan.-Mar. 1960.

[3] Kerns, D. M. Correction of near-field antenna measurements made with an arbitrary but known measuring antenna. Electron. Lett. 6: 346-347; May 1970.

[4] Kerns, D. M. New method of gain measurement using two identical antennas. Electron. Lett. 6:347-349; May 1970.

[5] Baird, R. C.; Newell, A. C.; Wacker, P. F.; Kerns, D. M. Recent experimental results in near-field antenna measurements. Electron. Lett. 6: 349-351; May 1970.

[6] Joy, E. B.; Paris, D. T. Spatial sampling and filtering in near-field measurements. IEEE Trans. Antennas Propagat. AP-20: 253-261; May 1972.

[7] Yaghjian, A. D. Upper-bound errors in far-field antenna parameters determined from planar near-field measurements, Part I: Analysis. Nat. Bur. Stand. (U.S.) Tech Note 667; 1975.

[8] Newell, A. C.; Crawford, M. L. Planar near-field measurements on high performance array antennas. Nat. Bur. Stand. (U.S.) NBSIR 74-380; July 1974.

[9] Kerns, D. M. Plane-wave scattering-matrix theory of antennas and antenna-antenna interactions: Formulation and applications. Nat. Bur. Stand. (U.S.) J. Res. 80(B): 5-51; Jan.-Mar. 1976.

[10] Newell, A. C.; Baird, R. C.; Wacker, P. F. Accurate measurement of antenna gain and polarization at reduced distances by an extrapolation technique. IEEE Trans. Antennas Propagat. AP-21(4): 418-431; July 1973.

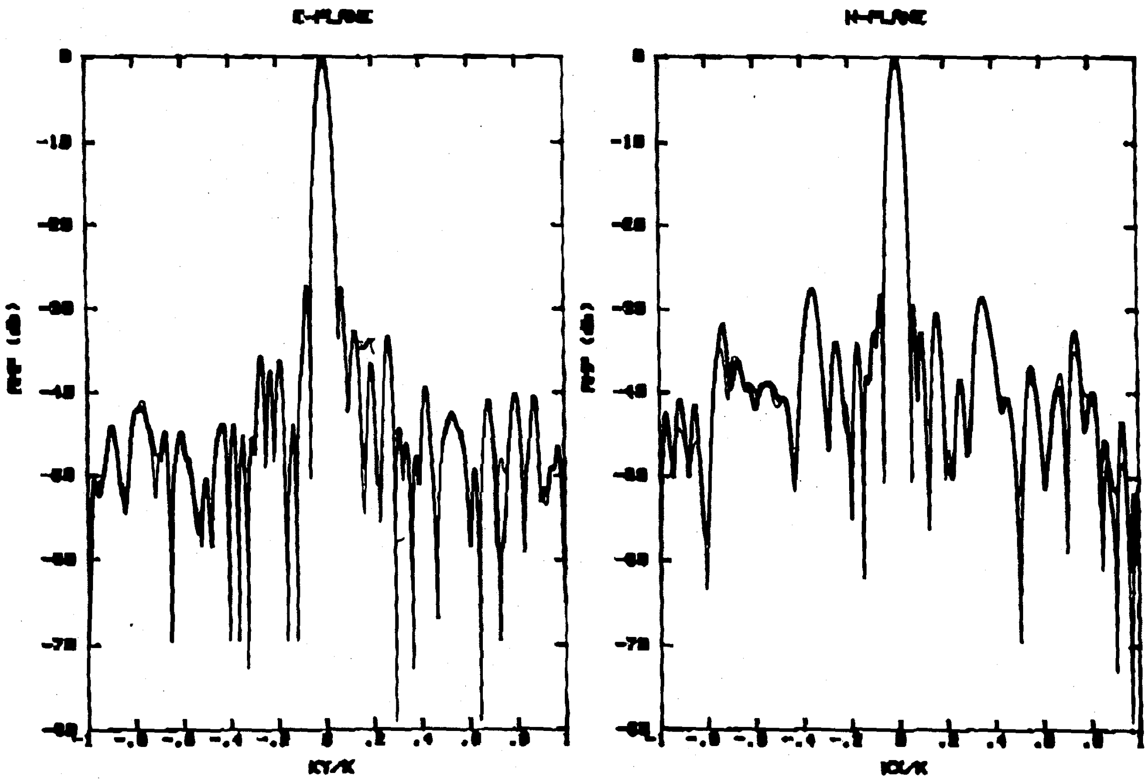

Figure 1. Comparison of principal far-field patterns; (a) E-plane, (b) H-plane; Main component: antenna transmitting pulsed-cw 1 (dark line), antenna transmitting cw (light line); d = 12 cm; 111 x 111 input array.

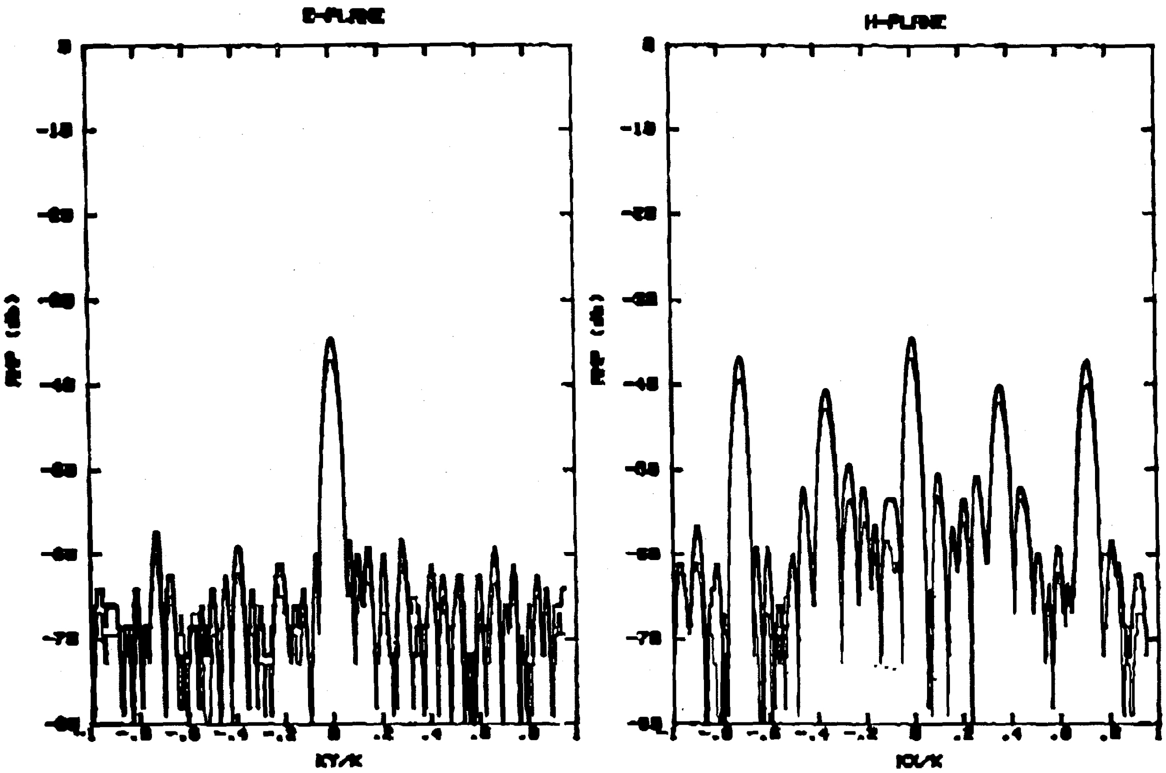

Figure 2. Comparison of principal far-field patterns; (a) E-plane, (b) H-plane; Cross component; antenna transmitting pulsed-cw 2 (dark line), antenna transmitting cw (light line); d - 12 cm; 111 x 111 input array.

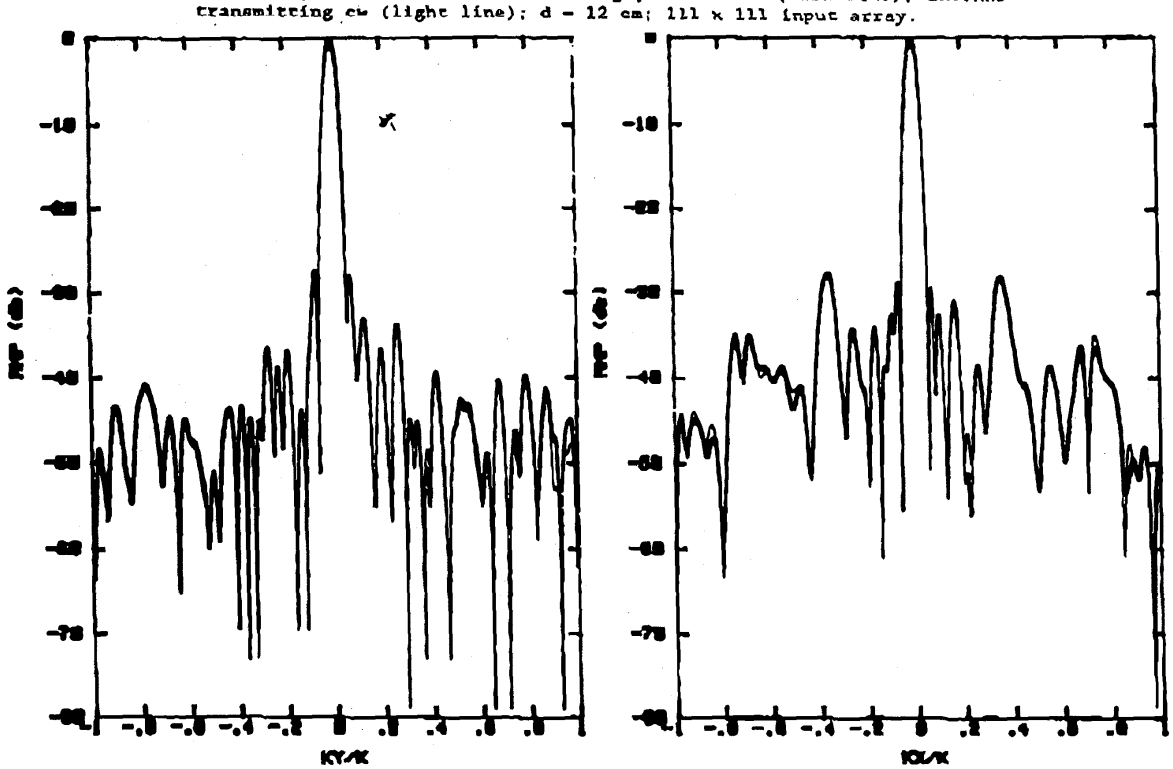

Figure 3. Comparison of principal far-field patterns: (a) E-plane, (b) H-plane: Main component; antenna transmitting cw (dark line), 143 x 143 input array, antenna transmitting cw (light line). 111 x 111 input array; d - 12 cm.

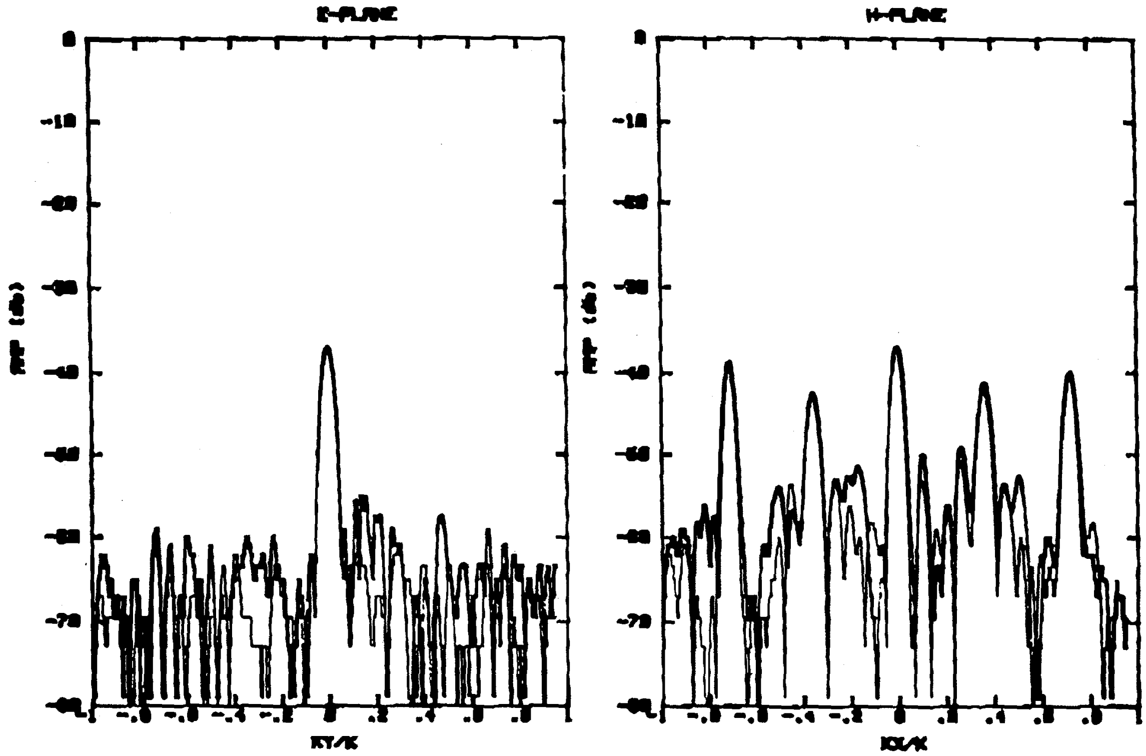

Figure 4. Comparison of principal far-field patterns: (a) E-plane, (b) H-plane; Cross component; antenna transmitting cw (dark line), 143 x 143 input array, antenna transmitting cw (light line), 111 x 111 input array; d = 12 cm.

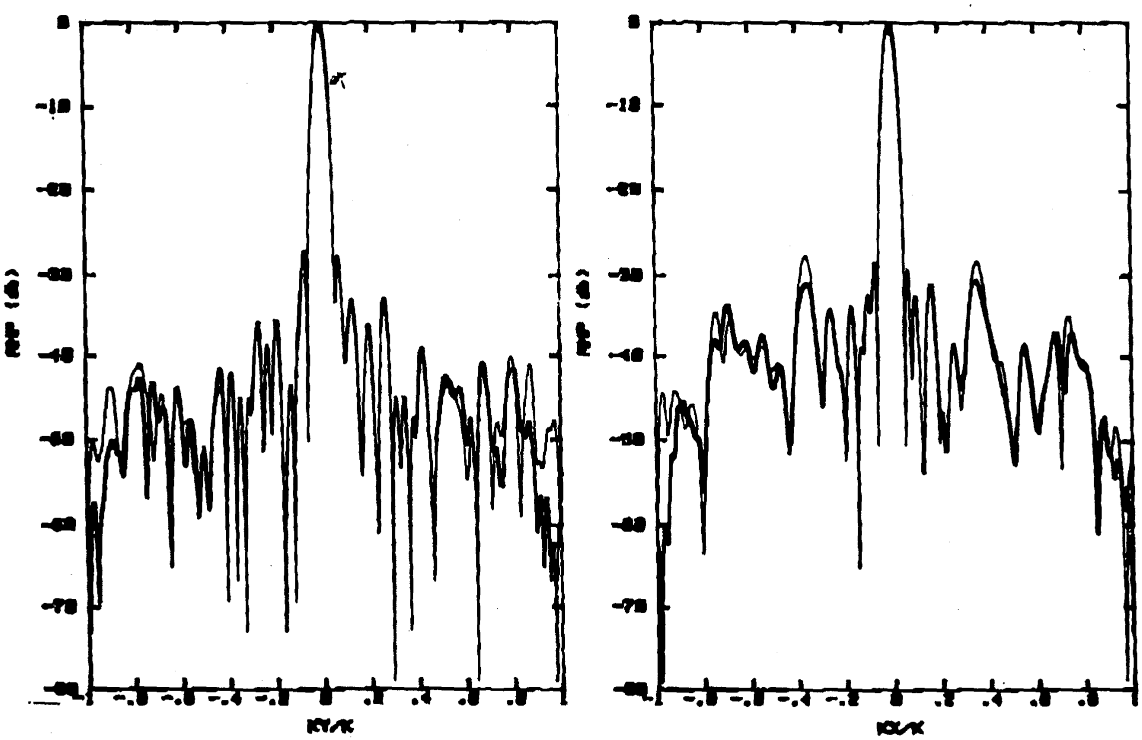

Figure 5. Comparison of principal far-field patterns; (a) E-plane, (b) H-plane; Main component; antenna transmitting cw (dark line), d = 30 cm; antenna transmitting cw (light line), d = 12 cm; 111 x 111 input array.

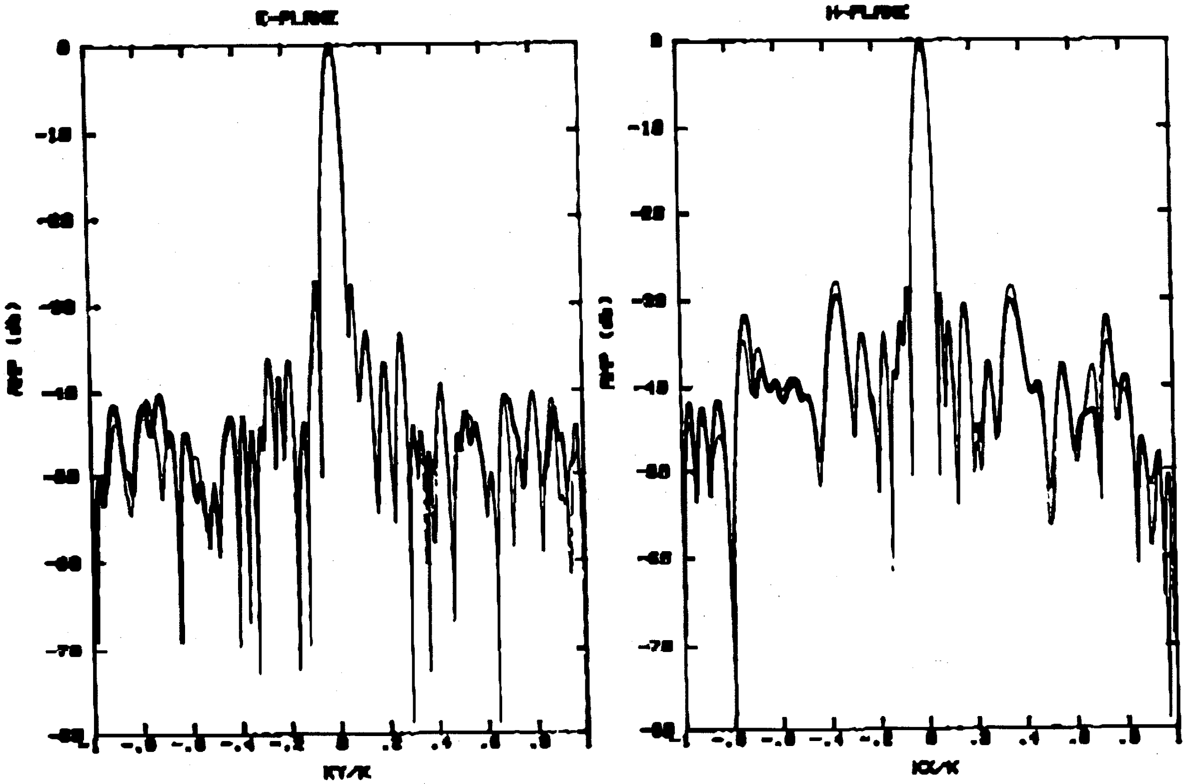

Figure 6. Comparison of principal far-field patterns: (a) E-plane, (b) H-plane: Main component; antenna transmitting cw (dark line), d = 12 + 1/8 lambda cm: antenna transmitting cw (light line), d = 12 cm: 143 x 143 input array.

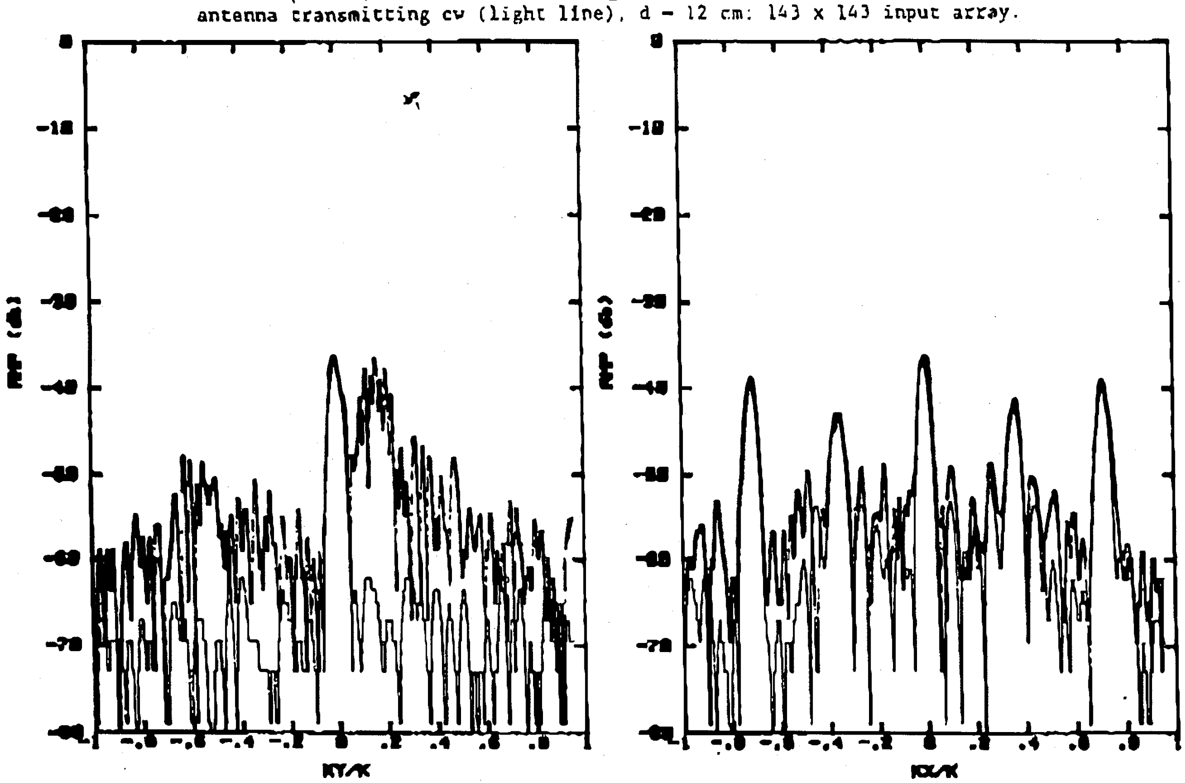

[illegible] of principal far-field patterns: (a) E-plane, (b) H-plane: [illegible] component; antenna transmitting pulsed-cw 1 (dark line), antenna [illegible] cw [illegible], [illegible] = 12 cm; 111 x 111 input array.

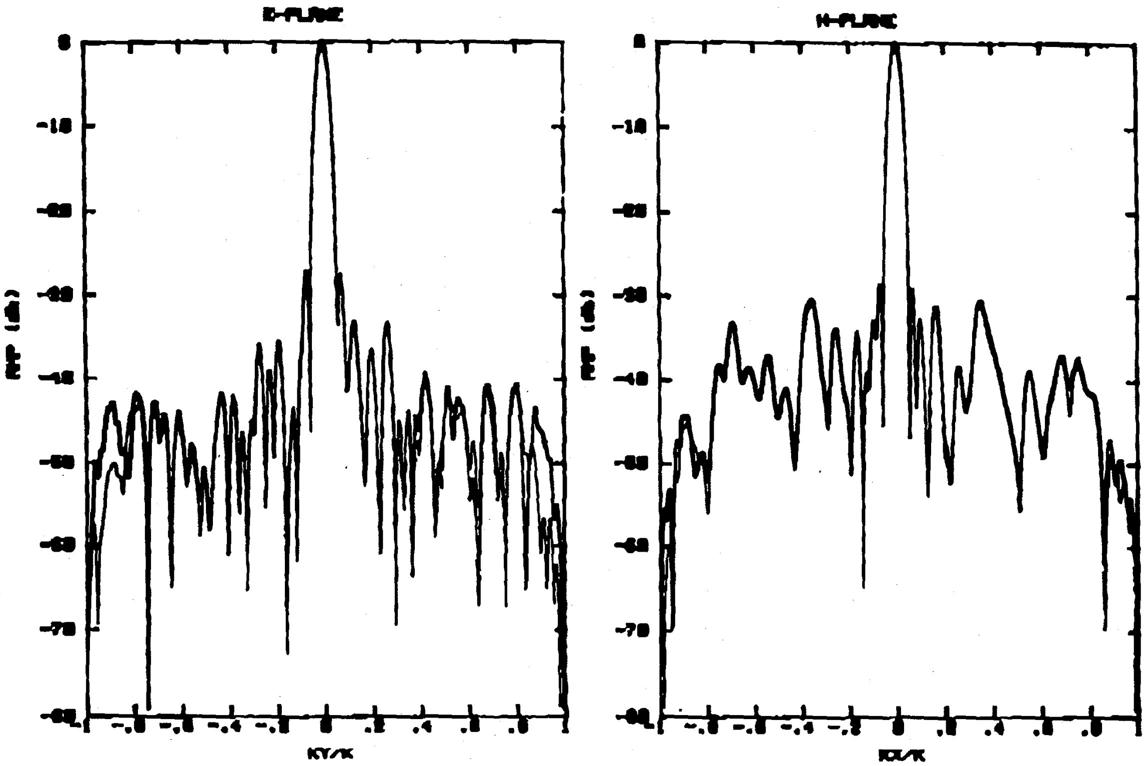

Figure 8. Comparison of principal far-field patterns: (a) E-plane, (b) H-plane;
Main component: antenna transmitting cw (dark line), 143 x 143 input array,
antenna transmitting cw (light line), 111 x 111 input array: d - 30 cm.

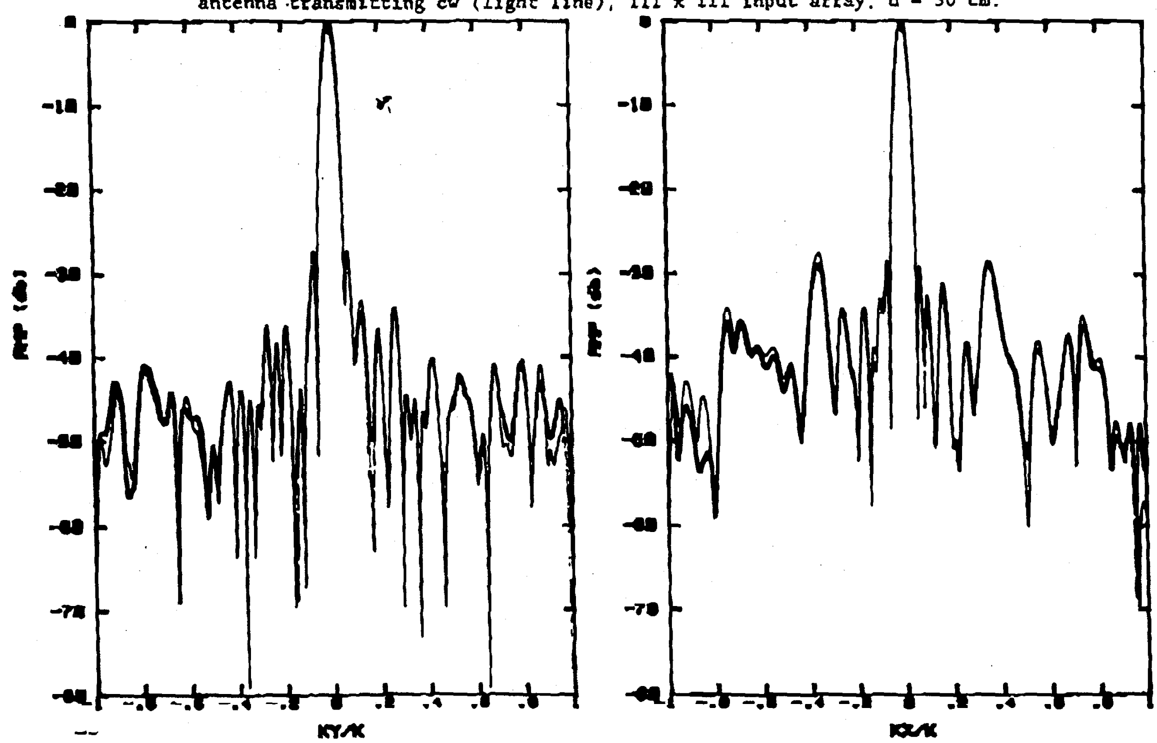

Figure 9. Comparison of principal far-field patterns; (a) E-plane, (b) H-plane;
Main component; antenna receiving cw measured at other facility (dark line),
antenna receiving cw (light line); d - 12 cm; 111 x 111 input array.